Proceedings World Geothermal Congress 2010
Bali, Indonesia, 25-29 April 2010

Conceptual Model for Coupling Geothermal Power Plants with Deep Reservoirs

G. Blöcher, S. Kranz, G. Zimmermann , S. Frick, A. Hassanzadegan, I. Moeck, W. Brandt, A. Saadat & E. Huenges

Helmholtz Centre Potsdam - GFZ German Research Centre for Geosciences, Telegrafenberg A6, 14473 Potsdam, Germany

bloech@gfz-potsdam.de

Keywords: reservoir engineering, enhanced geothermal systems, geothermal power plant, coupled simulation

ABSTRACT

During geothermal power production the hydro-mechanical-thermal conditions of a geothermal reservoir will vary. Temperature and pore-pressure variations lead to a change of the reservoir properties such as porosity, permeability, electric conductivity and fluid properties. The variations are dependent on input and output parameters of the geothermal power plant such as the injection temperature and flow rate of the thermal water. The simulation of geothermal power plants and the reservoir behavior are usually treated separately, leading to a strong simplification of the interactions between both systems. Therefore a holistic approach including a reservoir-power plant coupling is necessary to predict the life cycle behavior and hence the cumulated electricity provision of the overall geothermal system.

We present a conceptual model, which is capable to combine all different aspects of geothermal power production including coupled processes. Power plant and geothermal reservoir are connected by injection and production wells, therefore changes of fluid properties due to heating and cooling inside the wells have to be taken into account. For this reason, interfaces between all model components such as geothermal power plant, boreholes and reservoir will be developed to simulate the circulation of the geothermal fluid inside the overall system. By means of a case study of the geothermal research site Groß Schönebeck, Germany, the application of the conceptual model will be presented taking into consideration a total operation time of 30 years.

1. INTRODUCTION

During the elapsed time of a geothermal project it became obvious, that for planning the well path and fracture design, for interpretation of hydraulic tests and stimulations as well as for prediction of reservoir behaviour and life cycle performance during the time of geothermal power production an appropriate numerical model becomes increasingly important.

To satisfy the requirements of the planned simulations the model should implement all the acquired knowledge of the reservoir, the injection and production well and the power plant. This includes the reservoir geology and structure and the geometry of wells and fractures. Further the hydraulic, thermal and mechanical processes inside the reservoir, the fluid flow inside the wells and inside the power plant must be captured.

Various simulation software exist, which can handle a part of the mentioned requirements, e.g. Eclipse (SCHLUMBERGER, 2008), Geosys (Korsawe et al. (2006), Wang and Kolditz (2007)) and Feflow (Diersch, 2005), can simulate the reservoir characteristics. Simulating the well behaviour, steady state and transient modelling tools have been developed e.g GEOWELLS (García-Valladares et al., 2006), HOLA (Bjornsson 1987) and WFSA (Hadgu and Freeston 1990).

For power plant modelling different software tools such as Aspen Plus, Ebsilon or IPSEpro are typically used (Giglmayer (2001). Also Dymola/Modelica (Casella et al., 2005) has started to being used in the last years.

At the moment no simulation software exists, which is capable to simulate all aspect of geothermal power generation. But, a combination of the available software, numerical and analytical approaches and empirical methods can close this gap. Therefore, we will present a conceptual model, which fulfil the requirements of a geothermal project.

2. CONCEPT

The principal concept is to combine the different aspects of geothermal power production by means of a complete system simulation. Therefore reasonable interface parameters between the different model part, which are power plant, injection and production well and reservoir have to be determined (figure 1). Further, a differentiation between input and output parameter must be defined. The required production rate $\dot{V}_{\mathrm{Rout}}$ from the reservoir is known in time. According to the pressure maintenance inside the power plant the outlet pressure p_{Pout} is adjusted and is specified during the total time of production.

Therefore, both parameters are used as input of the simulation. Based on the extracted water volume, the reservoir model can calculate the outlet pressure p_{Rout} and the outlet temperature T_{Rout}. By means of these boundaries and pressure p_{Pin} the pressure change Δp_1 and temperature change ΔT_1 across the production well is calculated. The pressure change is due to friction loss, density change of the water column and production rate. The temperature change inside the production well is controlled by conductive heat loss to the surrounding rocks only. At the surface, the temperature of the thermal water is reduced by heat transfer $\dot{Q}$ from the thermal water cycle to the power plant cycle. Further, the pressure inside the surface facility will decrease according to an additional friction loss. The specified outlet pressure p_{Pout} will be adjusted to a suitable injection pressure. Therefore, the injection pump performance $\dot{W}_{Pump2}$ must be taken into account. The processes inside the injection well are similar to those of the production well and the injection rate $\dot{V}_{Rin}$, temperature T_{Rin}, pressure p_{Rin} will be determined. The temperature change ΔT_4 and pressure changes Δp_4 inside the reservoir will be analyzed by finite element subsurface simulation.

For modeling the complete system in particular for determination of friction loss inside the pipes and wells and for the hydraulic conductivity of the reservoir, density ρ

and dynamic viscosity μ are the key properties. These properties depend on temperature and pressure as follows:

$$\rho = \rho_0 \left[1 - \beta(T - T_0) + \gamma(p - p_0)\right], \quad (1)$$

with thermal expansion coefficient β and compressibility γ are all related to temperature and pressure (Magri et al., 2005) and

$$\frac{1}{\mu} = \frac{1 + 0.7063\varsigma - 0.04832\varsigma^3}{\mu_0}, \quad (2)$$

with ς =(T-150)/100 at T in °C (Mercer and Pinder, 1974).

For modelling the heat flow in particular for the conductive part the heat capacity c and the heat conductivity λ are the most significant values. Changes of heat capacity of the fluid are marginal until temperatures of 200°C at atmospheric pressure and can be taken as constant (McDermott et al., 2006). Values of the heat conductivity can be determined by laboratory experiments at 20°C and will be corrected by its temperature dependence. The functional relation is given by (Somerton, 1992):

$$\lambda = \lambda_{20} - 10^{-3}(T - 293)(\lambda_{20} - 1.38) *$$

$$(\lambda_{20}(1.8 * 10^{-3} T)^{-0.25\lambda_{20} + 1.28})\lambda_{20}^{-0.64}, \quad (3)$$

where λ_{20} denotes the heat conductivity measured at 20°C by laboratory experiments. By means of the equation of state above we are able to calculate the heat conductivity, density and the dynamic viscosity of the fluid at any point of the thermal water cycle.

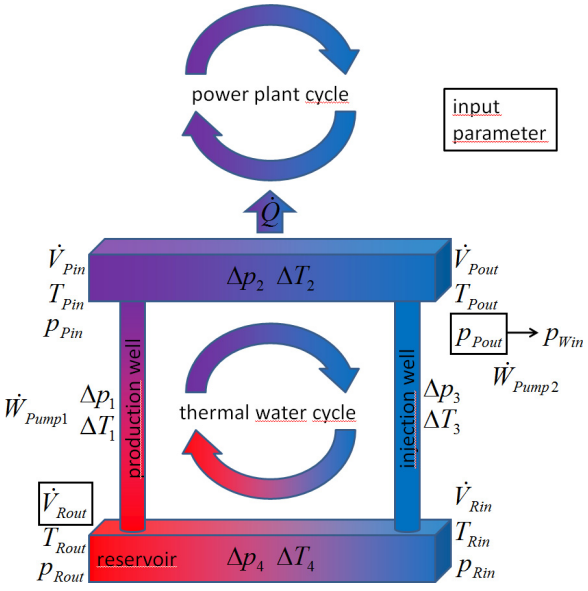

Figure 1: Schematic model of thermal water cycle and power plant cycle. The thermal water cycle simulation consists of a reservoir model, an injection and production well simulation and a link to the surface power plant model

2.1 Partial Model Reservoir

The governing equation of this thermohaline convection in a saturated porous are derived from the conservation principles for linear momentum, mass and energy (Bear and Bachmat (1990), Kolditz et al. (1998)) and the resulting system is given by the following set of differential equations:

$$S_s \frac{\partial h}{\partial t} + \frac{\partial q_{fi}}{\partial x_i} = Q_\rho \quad (4)$$

there S_s, q_{fi} and Q_ρ denote specific storage coefficient, Darcy velocity vector and source/sink function of the fluid, respectively. The Darcy velocity vector can be expressed in terms of hydraulic conductivity tensor K_{ij}, fluid viscosity relation function f_μ and fluid density ρ_f:

$$q_{fi} = -K_{ij} f_u \left(\frac{\partial h}{\partial x_j} + \frac{\rho_f - \rho_{f0}}{\rho_{f0}} e_j \right) \quad (5)$$

Without adsorption of the solute at the solid surface the source/sink of the contaminant mass Q_C is calculated as sum of mass storage, convection, and diffusion (Fickian law):

$$\frac{\partial}{\partial t}(\phi C) + \frac{\partial}{\partial x_i}(q_{fi} C) - \frac{\partial}{\partial x_i}(D_{ij} \frac{\partial C}{\partial x_j}) = Q_C \quad (6)$$

where C is the mass concentration, D the hydrodynamic dispersion and φ the porosity. The heat supply Q_T is the sum of heat storage, convection and conduction (Fourier's law) and is determined by means of heat capacity c of the fluid and solid, thermodispersion tensor λ_{ij} (conductive and dispersive part) at certain temperature T:

$$\frac{\partial}{\partial t}[(\phi\rho_f c_f + (1-\phi)\rho_s c_s)T] + \frac{\partial}{\partial x_i}(\rho_f q_{fi} c_f T) - \frac{\partial}{\partial x_i}\left(\lambda_{ij} \frac{\partial T}{\partial x_j}\right) = Q_T \quad (7)$$

2.2 Partial Model Well

The fluid flow in the well is calculated considering fluid mechanics and heat transfer methods applicable for vertical pipe fluid flow. The hydraulic and thermal well modelling is based on the mass, momentum and energy conservation laws considering the following assumptions:

- one dimensional, transient fluid flow
- one phase flow is considered
- calculation of thermo and physical fluid properties according appropriate correlations
- heat exchange inside the well is calculated using empirical correlations

The governing equations are formulated to describe fluid flow inside a control volume. For each control volume the change in mass, pressure and energy is calculated.

2.2.1. Conservation of Mass

$$\frac{d\dot{m}}{dz} = -\frac{dm}{dt} = \frac{d(\rho S dz)}{dt} \quad (8)$$

S indicates the control volume area perpendicular to the fluid flow and dz indicates the length of control volume in the direction of the well path.

2.2.2 Momentum Conservation

By means of the conservation law of momentum the pressure change between inlet and outlet of each control volume is calculated.

$$\Delta p = -\left(\frac{\Delta z}{S}\right)\cdot\left[\left(f\,\frac{\overline{\rho u}^2}{2D_h}\right)+(\rho S g\sin\delta)+\left(\frac{\Delta(\dot{m}u)}{\Delta z}\right)+\left(\frac{\Delta\dot{m}}{\Delta t}\right)\right] \quad (9)$$

The terms in brackets denote the friction loss, gravitational effect considering a declination angle δ and effect of acceleration. The last term represents the transient pressure effect due to a changing density in the time period Δt. The friction factor f is calculated according the flow regime, laminar or turbulent.

Considering laminar flow that means Re<2000, the friction factor is derived from Hagen-Poiseuille flow regime and yields to:

$$f = \frac{16}{\mathrm{Re}_{Dh}}, \text{ with } \mathrm{Re}_{Dh} = \frac{u\cdot D_h}{\upsilon} \quad (10)$$

Considering turbulent pipe flow that means $4\cdot10^3 \le \mathrm{Re} \le 10^8$, the explicit Colebrook-White formula taking into account the pipe surface conditions (roughness k_s or relative roughness k_s/D) is applied.

$$f = \frac{0.25}{\left[\log_{10}\left(\frac{k_s}{3.7\cdot D}+\frac{5.74}{\mathrm{Re}^{0.9}}\right)\right]^2} \quad (11)$$

valid for: $10^{-5} \le \frac{k_s}{D} \le 2\cdot10^{-2}$

2.2.3 Energy Conservation

By means of the energy conservation law the enthalpy at the outlet of each control volume is calculated.

$$d(\dot{m}e) = -\frac{d(me)}{dt} - \dot{q}\pi D_h dz - S dz\frac{dp}{dt} - \frac{d(pu)}{dz} - \frac{d(\tau u)}{dz}, \quad (12)$$

with $e = \left(h+\frac{1}{2}u^2+g\,z\sin\delta\right)$

The heat loss occurring while fluid flow inside the well pipe is calculated considering fully developed thermal and flow velocity profiles inside the well pipe. That means, fluid condition at the well inlet are neglected because of the very small diameter to length ratio of the well.

The calculation of the local heat transfer coefficient *h* at the inner pipe wall is distinguished according the flow regime: laminar or turbulent. For laminar fluid flow the following equation is used.

$$Nu = \frac{\alpha\cdot D_h}{\lambda} = 3.657 \quad \text{valid for} \quad \mathrm{Re}<2300,\ \mathrm{Pr}>0.6,$$
$$\mathrm{Re}\cdot\mathrm{Pr}\cdot\frac{L}{D} > 0.05,\ \mathrm{Pr} = \frac{\mu\cdot c_p}{\lambda}, \quad (13)$$

where μ, c_p, λ, α, D_h are the dynamic viscosity (kg/ms), specific heat capacity (kJ/kgK), thermal conductivity (W/mK), the local heat transfer coefficient (W/m²K) and the pipe diameter (m)

Considering transition and turbulent flow the heat transfer coefficient is estimated using the following equation according Gnielinski (1976):

$$Nu = \frac{(f/8)\cdot(\mathrm{Re}-1000)\cdot\mathrm{Pr}}{1.00+12.7\cdot(f/8)^{1/2}\cdot\left(\mathrm{Pr}^{2/3}-1\right)}, \quad (14)$$

with $f = [1.82\cdot\log(\mathrm{Re})-1.64]^{-2}$,

valid for $2300 < \mathrm{Re} < 5x10^6$ and $1.0 < \mathrm{Pr} < 10^6$.

Using the estimated heat transfer coefficient α the heat flow at the inner pipe wall $\dot{q}$ is calculated as follows: $\dot{q} = \alpha\cdot(T_f - T_{wall})$ where T_f and T_{wall} are the fluid temperature of the control volume and the pipe wall temperature. T_{wall} is considered as constant for each control volume.

2.2.4 Heat transfer at well-rock interface

The heat transfer through the pipe wall and the rock is calculated using a finite element model. Here, the above mentioned local heat transfer coefficient at the inner pipe wall serves as boundary condition for the heat transfer calculation. On the other hand the wall temperature is given by the finite element model.

2.3 Partial Model Power Plant

The power plant partial model is a quasi-stationary model which contains the surface part of the thermal water loop and the power conversion in a binary cycle (figure 2). In order to consider varying operational conditions part load behavior will be considered. The modeling approach is simplified outlined in the following.

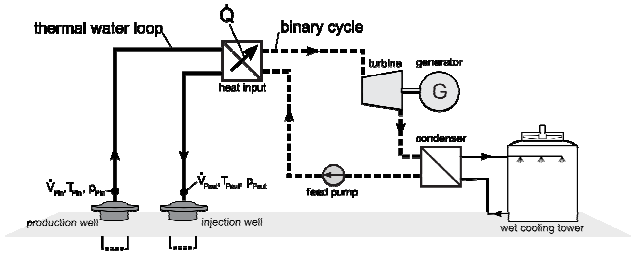

Figure 2: Schematic set-up of power plant partial model including thermal water loop on the surface and power conversion in a binary unit

The pressure difference Δp_2 is based on friction losses in the surface part of the thermal water loop are calculated according to the same approach as applied for wells. Friction losses occur in the pipe, bends and armatures such as heat exchangers or filters.

The temperature difference ΔT_2 is derived from the energy balance around the heat transfer between thermal water and the binary cycle.

$$\dot{Q} = \dot{m}_{Pin} c_p (T_{Pin} - T_{Pout}), \quad (15)$$

where $\dot{m}_{Pin}$ and c_p are mass flow based on $\dot{V}_{Pin}$, T_{Pin} and p_{pin} and specific heat capacity of thermal water. The binary cycle contains a pure low-boiling working fluid (e.g. isobutane) which is preheated, evaporated and in some cases superheated. It is designed for a specific operational point with following data:

- evaporation temperature T_v,
- steam quality of the live vapour x_v,
- condensing temperature T_c, and
- nominal working fluid mass flow $\dot{m}_{WF,nom}$

For the design point the heat transfer can be written as:

$$\dot{Q}_{nom} = \dot{m}_{WF,nom}(h_v - h_{pc}) , \quad (16)$$

where h_v and h_{pc} is the enthalpy of the live vapour and the pressurised condensate respectively. The enthalpy of the working fluid at a specific state is derived from a thermo-physical data base and is determined by temperature T_i, pressure p_i and in the vapour-liquid-region by steam quality x_i.

The net power obtained at the designed point P_{el} is then:

$$P_{el} = \dot{m}_{WF,nom}(h_v - h_{vout,s}) \eta_i \eta_m - P_{aux} , \quad (17)$$

where $h_{vout,s}$, η_i, η_m, and P_{aux} are enthalpy of the exhaust steam of a isentropic expansion to the condensation pressure, nominal isentropic turbine efficiency, mechanical efficiency of the turbine-generator-unit and consumed auxiliary power. Auxiliary power consuming components are the feed-pump, cooling pumps and fans in the recooling system (e.g. wet cooling tower), and down hole pump and injection pump.

Under part load conditions load-dependent behaviour of the different plant components is considered. Components such as pumps, fans but also the mechanical performance of the turbine are accounted with load-dependent efficiencies. For the part load behavior of the turbine the isentropic efficiency is adapted according to Mühltaler (2001):

$$\eta_i = \eta_{i,nom} (1 - \alpha_T \left(\frac{\Pi_{nom}}{\Pi} - 1 \right)^2) , \quad (18)$$

where $\eta_{i,nom}$, α_T, Π_{nom} and Π are isentropic turbine efficiency at the design point, efficiency factor and pressure ratio of the turbine at the design point and operation point respectively.

Regarding the heat transfer load-dependent transmission coefficients are considered. Dividing the heat input to the binary cycle, for example, into the different modes of heat transfer:

$$\dot{Q} = \dot{Q}_p + \dot{Q}_e + \dot{Q}_s , \quad (19)$$

where $\dot{Q}_p$, $\dot{Q}_e$ and $\dot{Q}_s$ are the heat transfer rate for pre-heating, evaporation and superheating respectively, the heat transfer rate of a specific application is calculated according to Cengel (2002) as:

$$\dot{Q}_i = U_{nom,i} \left(\frac{\dot{m}_{WF}}{\dot{m}_{WF,nom}} \right)^{f_U} A_i \, \Delta T_{m,i} , \quad i = p,e \text{ or } s \quad (20)$$

where $U_{nom,i}$, $\dot{m}_{WF}$, f_U, A_i and $\Delta T_{m,i}$ are the nominal heat transmission coefficient of the heat exchanger at the design point, working fluid mass flow, part load factor, heat transfer area and mean temperature difference in the heat exchanger.

3. CASE STUDY GROß SCHÖNEBECK

The technical feasibility of geothermal power production will be demonstrated by means of a borehole doublet system consistent of a production and injection well at the geothermal research site Groß Schönebeck (40 km north of Berlin/Germany).

The reservoir is located within the Lower Permian of the North East German Basin between -3815 m and -4247 m true vertical depth subsea (TVDSS). The reservoir rocks are classified into two rock units from base to top: volcanic rocks (Lower Rotliegend of the Lower Permian) and siliciclastics (Upper Rotliegend of the Lower Permian) ranging from conglomerates to fine grained sand-, silt- and mudstones. These two main units are sub-classified depending on their lithological properties (table 1), which is in particular of importance for the hydraulic-thermal-mechanical (HTM) modeling: Due to the high hydraulic conductivity and porosity, the Elbe base sandstone I and II are the most prominent horizons for geothermal power production.

Table 1. Nomenclature for geological formations of Groß Schönebeck reservoir, including lithology and vertical dimension (true vertical depth sub-sea (TVDSS)).

Unit	Lithology	Top	Bottom
Hannover formation	silt- and mudstone	-3815	-3974
Elbe alternating sequence	siltstone to fine grained sandstone	-3974	-4004
Elbe base sandstone II	fine grained sandstone	-4004	-4059
Elbe base sandstone I	fine to medium grained sandstone	-4059	-4111
Havel formation	Conglomerates from fine sandstone to fine grained gravel	-4111	-4147
Volcanic rocks	Ryolithe and Andesite	-4147	-4247

The intended injection well E GrSk3/90 was tested to investigate scenarios of enhancing productivity of thermal fluid recovery from the underground (Legarth et al. (2005), Reinicke et al. (2005), Zimmermann et al. (2005)). The doublet system was completed by a second well Gt GrSk4/05 with a total depth of -4198 m in 2007, followed by three stimulation treatments to enhance productivity.

In order to increase the apparent thickness of the reservoir horizon, the production well was inclined in the reservoir section by 48° and was drilled in the direction of the minimum horizontal stress (Sh = 288° azimuth) for optimum hydraulic fracture alignment in relation to the stimulated pre-existing well E GrSk3/90. Hence the orientation of the fractures will be 18° azimuth in the

direction of the maximum horizontal stress (Holl et al., 2005).

In the present study we will describe, how to set-up a combined model for enhanced geothermal systems (EGS) and we will discuss two different aspects. First we will show how to combine a power plant, well and reservoir model and second we will interpret the life-cycle performance of the geothermal research doublet at the drill site Groß Schönebeck by means of new simulation technology.

3.1 Partial Model Reservoir

3.1.1 Stationary State

In preparation of a dynamic reservoir simulation the initial reservoir conditions have to be determined. These are the initial hydraulic heads, temperature field and the total dissolved solids. For this purpose we modeled the steady state condition of the natural reservoir without any injection and production. For this model we set the initial hydraulic head to h(xi; t0) = -185 m for the total domain and assigned two no flow boundaries q_h(xi; t) = 0 m/s at north-east and south-west borders of the reservoir. These two borders represent two natural fault systems which are non conductive in the recent stress field (Moeck et al., 2008). The initial temperature T(xi; t_0) was set to 137.5°C for the total domain, representing the temperature at the top of the reservoir. For the top layer we applied a 1st kind boundary condition by setting a constant temperature of T(xi; t) = 137.5°C for the total time of simulation. Further, a terrestrial heat flow of q_T (xi; t) = 72 mW/m² was applied at the bottom surface. For the mass concentration we used 265 g/l as start value and no further boundary conditions were set.

The initial time step length of the model is 1e-08 days and the final time was set to 100000 years. After approx. 40000 years quasi stationary conditions were archived. The resulting temperature profile is shown in figure 3 and is consistent with measured data. Only for the volcanic rocks the calculated temperature gradient is lower than the measured one. This could be due to the fact that the assumed heat conductivity is too high. In contrast, the modeled static water level h = -191 m at E GrSk3/90 matches the measured one h = -182.8 to -196.3 m very well (Huenges and Hurter, 2002).

3.1.2 Transient State

Based on the results of the stationary model we started with the adjustment of the transient model. For the initial conditions for hydraulic head, temperature and concentration the calculated values of the stationary model were chosen. In addition we removed the 1st kind boundary condition at the top layer, which was a constant temperature of T(xi; t) = 137.5°C and added a constant temperature of T(xi; t) = 70°C along the injection well. This boundary condition represents the temperature of the injected fluid during the total time of simulation. The final simulation time was set to 30 years, according to the expected life-cycle of geothermal use.

Further, we applied a constant injection rate of Q(xi; t) = 75 m³/h at the top of the Elbe base sandstone II unit, which corresponds which the top of the multifrac. At the production well a constant production rate of Q(xi; t) = -75 m3/h was set at the top of the Elbe alternating sequence unit and therefore at the top at the 2nd gel-proppant frac. Due to the fact, that the extracted fluid will be reinjected after passing the heat exchanger, we set the mass concentration to C(xi; t) = 265 g/l at the injection point.

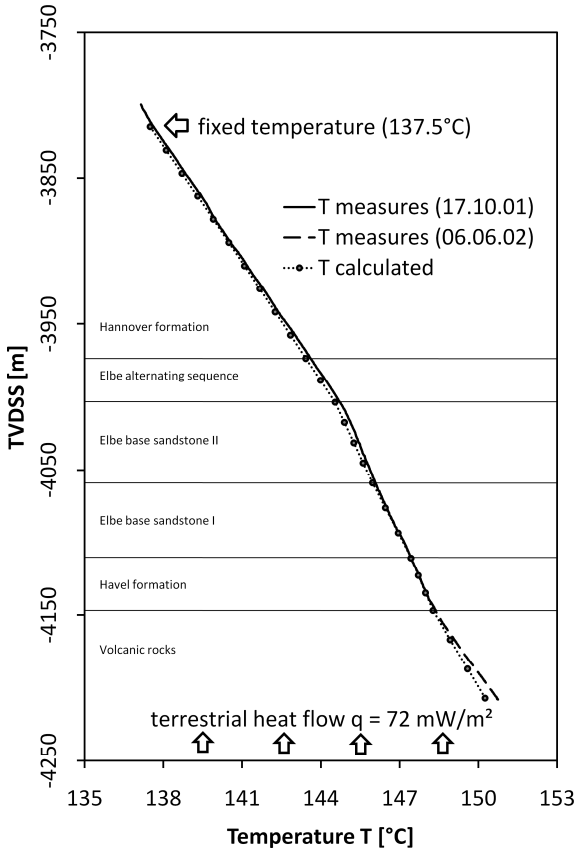

Figure 3: Temperature profile of the reservoir at the injection well E GrSk03/90. The observed field data (solid line) and simulated temperature (doted line) properly match together

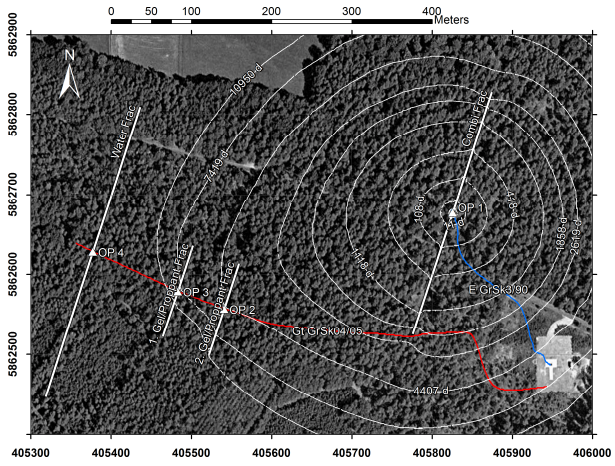

Figure 4: Chronological sequence of the propagation of the 130°C temperature front after start of injection at Elbe base sandstone I. Also shown is the projection of the drill site Groß Schönebeck including injection and production well and induced hydraulic fractures

After starting of reinjection of the saline water with a temperature of T = 70°C, the cold water front starts propagating around the injection well. In figure 4 different propagation states of the 130°C isosurface during the 30

years (10950 d) operation time are shown. It is obvious that the injected fluid first flows along the induced multifrac and afterwards infiltrates the rock matrix. Here, the high permeable rock units of the Elbe base sandstones are passed best. After passing the rock matrix the injected fluid reaches the 2nd gel-proppant frac (308 m away from the injection well) first. Due to the high hydraulic conductivity of the induced fracture, the fluid is directly forwarded to the production well before the cold water bubble interferes with the production well. After approx. 3.6 years the cold water arrives the second gel-proppant frac and after approx. 5 years the first gel-proppant frac (352 m away the injection well) is hit by the cold water. The water frac (448 m away the injection well) is not reached by the 130°C isosurface but the cooling starts after approx. 10 years as well.

3.2 Partial Model Well

In this simulation the three-dimensional geometry of the subsurface domain describing the reservoir porous matrix structure was interconnected to one-dimensional features representing the injection and production well.

Different laws of fluid motion within the wells can be defined, e.g., Darcy, Hagen-Poiseuille or Manning-Strickler laws (Diersch, 2002). In the present study Hagen-Poiseuille law was applied. Both the geometric and physical characteristics of injection and production well were added to this simulation. The geometry of both wells was simplified by a vertical tube with a diameter of 5''. To avoid an advective heat transfer between well and reservoir matrix, the porosity around the wells was set to zero and the permeability was set infinitesimal small. Therefore, the temperature change inside the injection and production well are due to conductive heat transfer only.

Further, we applied a constant injection rate of Q(xi; t) = 75 m³/h at the top ground surface and at the production well a constant production rate of Q(xi; t) = -75 m3/h in 1000m depth, representing the position of the production pump. The final simulation time was set to 30 years, according to the expected life-cycle of geothermal use.

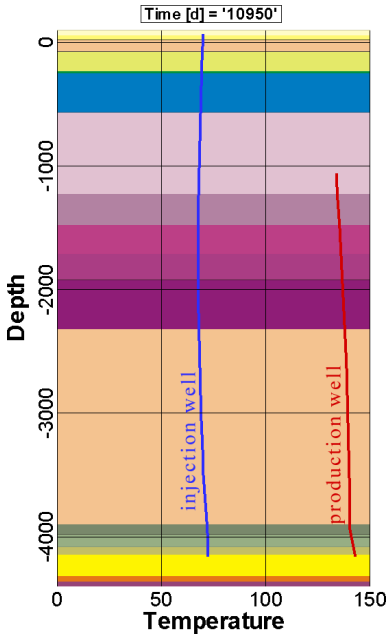

Figure 5: Simulated temperature profile along the injection and production well after 30 years operation

In figure 5 the temperature along the injection and production well at the final simulation time are shown. At the production side the inlet temperature in 4000m depth is 140°C. According to the conductive heat loss, the temperature decreases from bottom to top and a production temperature of 135°C at the production pump was observed. At the injection side the inlet temperature at the surface was set constant to 70°C. According to the natural geothermal gradient, the temperature of the rock matrix between 0 and 2000 m depth is lower than in the well. Therefore a decrease of the injection temperature to 68°C was observed. In higher depth the rock temperature is above the fluid temperature within the well and an increase of the injection temperature was simulated. By means of this simulation we determined an outlet temperature of 72°C at the injection well.

3.3 Partial Model Power Plant

The influence of the interface values defined in section 2 on the power output will be shown in the following at the example of a theoretical case study. The power plant model outlined in section 2.3 has therefore been applied for a virtual design point based on following assumptions:

reservoir temperature	150 °C
reservoir depth	4,000 m
specific heat capacity thermal water	3.5 kJ/kg K
productivity index	30 m^3/(h MPa)
injectivity index	30 m^3/(h MPa)
pore pressure gradient	10.7 bar/100 m

The binary unit is a basic Rankine cycle using isobutane as working fluid and being recooled by a forced draught wet cooling tower (Figure 2). It is designed for a inlet temperature of the thermal water equal to the reservoir temperature, a thermal water mass flow of 75 kg/s, an evaporation temperature of 101 °C and a condensation temperature of 28 °C (assuming an annual average ambient temperature of 15 °C and an average relative humidity of 76 %). The live vapor driving the turbine is saturated steam. Based on these parameters the working fluid mass flow is derived from the energy balance around the heat transfer between thermal water and working fluid. The resulting temperature of the thermal water at the outlet of the binary unit is 65 °C. Accounting the auxiliary power consumption of the down-hole pump (an injection pump is not needed under the conditions assumed here), the feed-pump in the binary unit and recooling system, the power output of this unit adds up to 1,240 kW. Component specifications such as pump efficiencies and temperature differences in heat exchangers are taken from Frick et al. (2010).

The influence of the interface values on the power output will be shown by means of a parameter variation. Part load behavior will not yet be considered.

The variation of the outlet temperature of thermal water, while keeping the other parameters constant unless not influenced by the outlet temperature, is shown in figure 6.

It can be seen that the power output reaches its maximum for the design point at 65 °C. This significant influence of T_{Pout} results from its oppositional influence on the conversion efficiency and transferred heat. A higher outlet temperature results in a higher evaporation temperatures and therefore also a higher conversion efficiency. However, less heat from the thermal is used.

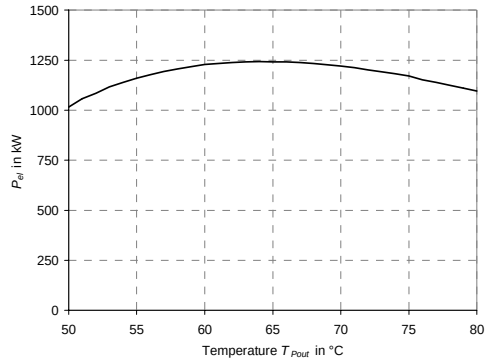

Figure 6: Influence of TPout on power output

In case the thermal water temperature at the inlet of the binary unit is not equal to the reservoir temperature, for example due to temperature losses in the production well, the power output decreases significantly (figure 7). This is reasoned by the resulting decrease of conversion efficiency and transferred heat.

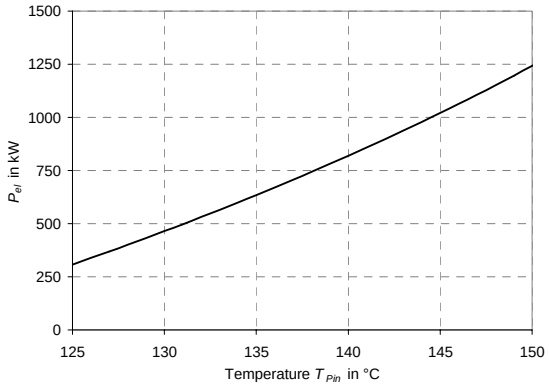

Figure 7: Influence of T_{Pin} on power output

Assuming that the reservoir pressure and accordingly its productivity index are lower or higher than expected or changes during operational life, the influence on the power output can be seen in figure 8. Even though the reservoir productivity has no influence on the produced gross power in the binary unit, the auxiliary power consumption of the down-hole pump is changed. The influence of the productivity thereby increases with decreasing productivity index.

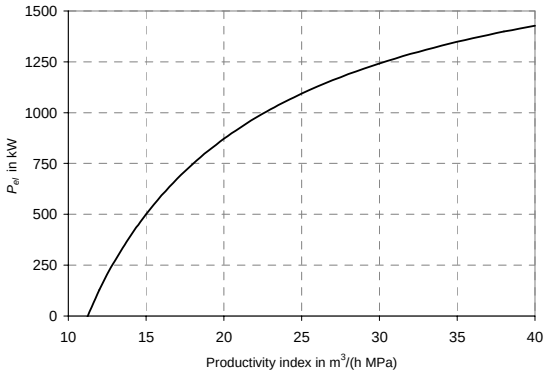

Figure 8: Influence of the productivity index on the power output

The influence for a varied mass flow rate of the thermal water for the assumed productivity can be seen from figure 9. Lower flow rates than the design flow rate of 75 kg/s thereby result in lower power output. Higher flow rates, in contrast, only lead to a higher power output only up to a flow rate of approximately 90 kg/s. This is due to the fact that with increasing flow rate not only the produced gross power increases but also the power consumption of the downhole pump. Since a higher flow rate also leads to a larger drawdown of the dynamic fluid level in the production well this influence is over-proportional.

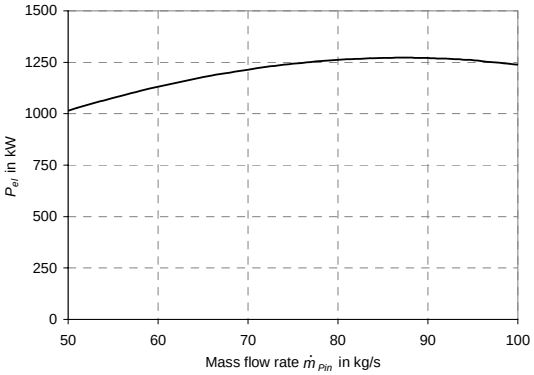

Figure 9: Influence of thermal water mass flow on power output

4. FUTURE WORK

The future work will be separated into two parts: the technical realization of coupling the different models and testing by using the example of Groß Schönebeck.

For the technical realization we will start with the integration of well bore model (pipe flow) into a reservoir model (fluid flow in porous media). Subsequently, an interface to the power plant model will be developed. For this purpose synchronization and an iterative exchange function between both simulations must be implemented.

The new simulation technology will be tested by means of Groß Schönebeck field data. We will perform sensitivity analyses of the total system. This can help to establish guidelines and recommendations for power plant and well design and reservoir management.

After successful testing the new simulation technology can be enhanced by implementation of chemical coupling, e.g. reactive transport, dissolution and precipitation and two-phase flow inside the wells and the surface thermal water loop.

CONCLUSION

We have shown, that each part of geothermal power production, which includes reservoir behavior, fluid flow inside production and injection well and processes inside the geothermal power plant are simulated separately.

But we also have shown, that in each separate simulation simplifications were made, which are non-negligible. In the reservoir model the temperature and pressure field and therefore the production temperature and production rate strongly depends on injection rate and injection temperature which were taken as constant.

By means of the power plant model we have shown that the electric power generation depends on productivity index, flow rate and inlet and outlet temperature. These parameters

are changing due to processes in the production and injection well and in the reservoir. But these changes were neglected in the present investigations.

Further, the temperature and pressure inside the wells will vary by conductive heat transfer and friction loss.

It becomes obvious, that all the components are linked together and cannot be handled separately. Therefore we conclude that for planning, interpretation, prediction and optimization of geothermal life cycle performance the complete system must be represented.

A combination of existing simulation tools will result in suitable modeling software. By means of this new approach all aspects of enhanced geothermal systems can be investigated in order to enhance life-cycle performance.

REFERENCES

Bear, J. and Bachmat, Y.: Introduction to Modeling of Transport Phenomena in Porous Media. Kluwer Academic Publishers. (1990).

Casella, F., Leva, A.: Object-Oriented Modelling & Simulation of Power Plants with Modelica: *Proceedings European Control Conference*, (2005). Sevilla, Spain.

Cengel, Y. A.: Heat Transfer: A Practical Approach. McGraw-Hill Higher Education. (2002)

Bjornsson, G.:A Multi-Feedzone Geothermal Wellbore Simulator, Phd Thesis, University of California, California (1987)

Diersch, H. J. G.: Feflow finite element subsurface flow and transport simulation system - user's manual / reference manual / white papaers. WASY Ltd, Berlin, Release 5.0. (2002).

Diersch, H. J. G.: Wasy software feflow; finite element subsurface flow and transport simulation system. Technical report, (2005). Institute for Water Resources Planning and Systems Research, Berlin, Germany.

Frick, S., Kranz, S. and Saadat, A.: Holistic Design Approach for Geothermal Binary Power Plants with Optimized Net Electricity Provision. *Proceedings World Geothermal Congress 2010*, (2010). Bali, Indonesia.

García-Valladares, O.; Sánchez-Upton, P. & Santoyo, E. Numerical modeling of flow processes inside geothermal wells: An approach for predicting production characteristics with uncertainties Energy Conversion and Management, 2006, 47, 1621 - 1643

Giglmayr, I: Modellierung von Kraft- und Heizkraftwerken, Vergleich von Software zur thermodynamischen Prozessrechnung. Fortschritt-Bericht VDI, Reihe 6 Energietechnik. VDI-Bericht 470, Düsseldorf, Germany (2001).

Gnielinski, V., 1976. New equations for heat and mass transfer in turbulent pipe and channel flow. Int.Chem. Engng 16, 359–368.

Hadgu, T. and Freeston, D.H.: A multi-purpose wellbore simulator, Geoth. Resour. Counc. Trans.14, (1990) 1279-1286

Holl, H. G., Moeck, I., and Schandelmeier, H.: Characterisation of the tectono-sedimentary evolution of a geothermal reservoir implications for exploitation (southern permian basin, NE germany). Proceedings World Geothermal Congress 2005 Antalya, (2005). Turkey, 24-29 April 2005, pages 1-5.

Huenges, E. and Hurter, S.: In-situ geothermielabor Groß Schönebeck 2000/2001: Bohrarbeiten, bohrlochmessungen, hydraulik, formationsfluide, tonminerale. Scientific technical report 02/14, (2002). GeoForschungsZentrum Potsdam, Germany.

Kolditz, O., Ratke, R., Diersch, H. J. G., and Zielke, W.: Coupled groundwater flow and transport: 1. verification of variable density flow and transport models. Adv Water Resources, (1998). 21:2746.

Korsawe, J., Starke, G., Wang, W. and Kolditz, O.: Finite Element Analysis of Poro-Elastic Consolidation in Porous Media: Mixed and Standard Approaches. *Computer Methods in Applied Mechanics and Engineering*, (2006). 10.1016/j.cma.2005.04.011, Volume 195, Issues 9-12 , 1 February 2006, Pages 1096-1115.

Legarth, B., Huenges, E., and Zimmermann, G.: Hydraulic fracturing in a sedimentary geothermal reservoir: Results and implications. International Journal of Rock Mechanics and Mining Sciences, (2005). 42:1028-1041.

Magri, F.: Mechanisms and fluid dynamics driving saline waters within the North East German Basin Results from thermohaline numerical simulations. PhD thesis, (2005). FU Berlin.

McDermott, C. I., Randriamanjatosoa, A. R., Tenzer, H., and Kolditz, O.: Simulation of heat extraction from crystalline rocks: The influence of coupled processes on differential reservoir cooling. Geothermics, . (2006). 35(3):321-344.

Mercer, J.W. and Pinder, G.F.: Finite element analysis og hydrothermal systems. Finite Element Methode in Flow Problems. Proc. 1st Symp., Swansea, (1974). (ed.Oden, J.T. et al.) Univ. of Alabama Press, 401.414.

Moeck, I., Schandelmeier, H., and Holl, H.-G.: The stress regime in a rotliegend reservoir of the northeast german basin. International Journal of Earth Sciences, (2008). ISSN 1437-3254.

Mühltaler, G: Anwendung objektorientierter Simulations-sprachen zur Modellierung von Kraftwerks-komponenten. Fortschritt-Bericht VDI, Reihe 6 Energietechnik. VDI-Bericht 450, Düsseldorf, Germany (2001).

Reinicke, A., Zimmermann, G., Huenges, E., and Burkhardt, H.: Estimation of hydraulic parameters after stimulation experiments in the geothermal reservoir Groß Schönebeck 3/90 (north-german basin). International Journal of Rock Mechanics and Mining Sciences, (2005). 42, 7-8:1082-1087.

SCHLUMBERGER: Eclipse, reference manual 2008.1. Technical report, Schlumberger Informations Solutions, Business Development Central and Eastern Europe, Hannover, Germany. (2008).

Somerton, W.: Thermal properties and temperature-related behavior of rock/fluid systems. Elsevier, (1992). 257.

Wang, W. and Kolditz, O.: Object-oriented finite element analysis of thermo-hydro-mechanical (THM) problems in porous media, *Int. J. Numerical Methods in*

Engineering, (2007). vol. 69 (1): 162-201, DOI:10.1002/nme.1770.

Zimmermann, G., Reinicke, A., Holl, H. G., Legarth, B., Saadat, A., and Huenges, E.: Well test analysis after massive waterfrac treatments in a sedimentary geothermal reservoir. In Proceedings World Geothermal Congress, (2005). Antalya, Turkey, 24-29 April 2005, 1-5.